Kinin B2 Receptor Mediates Induction of Cyclooxygenase-2 and Is Over-Expressed In Head and Neck Squamous Cell Carcinomas

Weiping Zhang[*], **Neil Bhola**[*], **Shailaja Kalyankrishna**[*], **William Gooding**[**], **Jennifer Hunt**[§], **Raja Seethala**[§], **Jennifer R. Grandis**[*,†,#], and **Jill M. Siegfried**[*,#]

[*]The Department of Pharmacology and Chemical Biology, the University of Pittsburgh Cancer Institute, 200 Lothrop Street, Pittsburgh PA 15213.

[†]The Department of Otolaryngology, the University of Pittsburgh Cancer Institute, 200 Lothrop Street, Pittsburgh PA 15213.

[**]The Department of Biostatistics, the University of Pittsburgh Cancer Institute, 200 Lothrop Street, Pittsburgh PA 15213.

[§]The Department of Pathology, the University of Pittsburgh Cancer Institute, 200 Lothrop Street, Pittsburgh PA 15213.

[#]University of Pittsburgh School of Medicine and the University of Pittsburgh Cancer Institute, 200 Lothrop Street, Pittsburgh PA 15213.

Abstract

Bradykinin (BK) has been shown to promote growth and migration of head and neck squamous cell carcinoma (HNSCC) cells via epidermal growth factor receptor (EGFR) transactivation. It has also been reported that BK can cause the induction of cyclooxygenase-2 (COX-2), a pro-tumorigenic enzyme, via the MAPK (Mitogen-Activated Protein Kinase) pathway in human airway cells. To determine whether COX-2 is up-regulated by BK in HNSCC, the current study investigated BK- induced EGFR transactivation, MAPK activation, and cyclooxygenase-2 (COX-2) expression in human HNSCC cells. BK induced a concentration- and time-dependent induction of COX-2 protein in HNSCC, which was preceded by phosphorylation of EGFR and MAPK. These effects were abolished by the B2 receptor (B2R) antagonist Hoe 140 but not the B1 receptor (B1R) antagonist, Lys-[Leu^8]des-Arg^9-BK. COX-2 induction was accompanied by increased release of PGE$_2$. No effect of a B1R agonist (des-Arg^9-BK) on p-MAPK or COX-2 expression was observed. B2R protein was found to be expressed in all four head and neck cell lines tested. Immunohistochemical analysis and immunoblot analysis revealed that B2R, but not B1R, was significantly over-expressed in HNSCC tumors compared to levels in normal mucosa from the same patient. In HNSCC cells, the BK-induced expression of COX-2 was inhibited by the EGFR kinase inhibitor gefitinib or mitogen activated protein kinase kinases (MEK) inhibitors (PD98059 or U0126). These results suggest that EGFR and MAPK are required for COX-2 induction by BK. Up-regulation of the B2R in head and neck cancers suggests this pathway is involved in HNSCC tumorigenesis.

Keywords

Bradykinin; B2 receptor; EGFR; MAPK; cyclooxygenase-2; head and neck cancer

Correspondence: Jill M. Siegfried, Ph.D, Department of Pharmacology, University of Pittsburgh,. E1352, 200 Lothrop Street, Pittsburgh, PA 15261. Siegfriedjm@upmc.edu.

INTRODUCTION

G-protein-coupled receptors (GPCR) have been shown to mediate growth of tumor cells in a variety of cancers including small cell- and non-small cell-lung cancer, prostate cancer and HNSCC. Some of the GPCRs implicated in this process include chemokine receptors, protease-activated receptors, and the receptors for thrombin, bradykinin (BK) and lysophosphatidic acid (1-5). GPCRs are desirable targets for drug development because of the availability of specific targeting agents for these receptors and the overexpression of these receptors in multiple tumor types (6). Hence there is considerable interest in targeting GPCRs as cancer therapy, alone or in combination with other targeting agents (7, 8).

BK is one of the GPCRs implicated in HNSCC tumorigenesis, wherein it promotes HNSCC cell migration and proliferation (8). Two types of BK receptors, B1 and B2 bradykinin receptors, have been implicated in tumorigenesis. For example, the B1 receptor (B1R) was upregulated in malignant prostate (9) and the B2 receptor (B2R) was overexpressed in human gliomas (10) and was detected in gastric, duodenal, lung and hepatic cancers (11). It has previously been determined which of the BK receptors are present in HNSCC tumors, whether they differ in expression relative to normal mucosal tissue, and which BK receptor contributes to HNSCC tumorigenesis. We therefore investigated the role of B1R and B2R in BK signaling in HNSCC.

GPCRs such as the BK receptor transactivate epidermal growth factor receptor (EGFR), utilizing the potent EGFR signaling pathways to mediate their effects (3). EGFR have been implicated in linking GPCRs to mitogen-activated protein kinase (MAPK) cascades, which mediate cell proliferative effects (8, 12). Our group has previously shown that in HNSCC cells, BK causes MMP-mediated release of TGFα, which transactivates EGFR, and that this pathway is dependent upon activation of src (8). Inhibition of EGFR kinase activity prevented BK-induced cell growth and migration of HNSCC, suggesting that EGFR autophosphorylation is required for this BK function in HNSCC (8). Other studies suggest that EGFR and MAPK are required for the proliferative effects of BK in breast and prostate cancer cells (13, 14). The specific BK receptor required to phosphorylate MAPK through EGFR in HNSCC cells is not known and was explored in this study.

In addition to causing HNSCC proliferation and migration (8), BK has been reported to induce other pro-tumorigenic proteins such as COX-2 in lung cancer cells (15). COX-2 is an important component of HNSCC tumorigenesis; it is overexpressed in HNSCC (16) and its catalyzed product PGE_2 is mitogenic for HNSCC (17). Unlike COX-1 which is constitutively present in many tissues, COX-2 is absent or present at very low levels under basal conditions, and is induced upon stimulation with growth factors or cytokines (18). A cooperative effect of blocking both EGFR and the COX-2 pathway has been observed both *in vivo* and *in vitro* in HNSCC (19). We hypothesized that BK induces COX-2 expression in HNSCC, mediated by activation of MAPK that is dependent upon EGFR cross-activation. Our data demonstrate that B2R is over-expressed in HNSCC, and that through this receptor, BK transactivates EGFR and utilizes the MAPK pathway to cause COX-2 induction. B2R over-expression in HNSCC may contribute to release of PGE_2, leading to tumor growth and invasion.

RESULTS

BK induces COX-2 expression in HNSCC cells

BK has been reported to induce expression of COX-2 in lung tumor cells (15). We tested whether BK also induces COX-2 in HNSCC cells. Three HNSCC cell lines (PCI-37A,

UM-22B, and 1483) were selected to study BK-induced COX-2 expression in a concentration- and time- dependent manner. Treatment of PCI-37A cells with increasing concentration of BK (0.1 ~1000 nM) for 2 h resulted in a concentration-dependent elevation of COX-2 expression. As little as 10 nM BK produced a maximum effect on COX-2 protein levels (2.3-fold increase, $P < 0.05$; Fig. 1A). At higher concentrations, a biphasic response was noted, with diminished COX-2 induction at BK treatments over 100 nM. Biphasic dose-responses have been noted in bioassays of BK activity (20). Biphasic responses are believed to be mediated by receptor phosphorylation, which shifts the affinity of kinase receptor for ligand and leads to receptor endocytosis (21). Treatment with 10 nM BK for increasing time periods also resulted in a time-dependent induction of COX-2 protein. COX-2 expression was increased by 10 min after BK addition and reached maximal levels by 2 ~ 4 h (3.8-fold induction, $P < 0.05$; Fig. 1B). BK induced a similar concentration-related increase in COX-2 expression in HNSCC cell lines UM-22B (3-fold increase, Fig. 1C, left panel, $P < 0.05$) and 1483 (2.4-fold increase, $P < 0.05$, Fig. 1C right panel). Three independent experiments were carried out for each condition. UM-22B cells, which contain lower B2R expression levels (see Fig. 6), were less sensitive to BK stimulation.

COX-2 induction has been frequently found to be caused by increased mRNA synthesis (22). We showed by RT-PCR analysis that COX-2 mRNA expression increased up to 2-fold over a 30 min and 2 h time period after BK treatment between 1 nM and 1μM. A biphasic response was also noted in mRNA induction, with diminished mRNA found at 1 μM compared to lower concentrations (see Supplemental Fig. 1A and 1B).

PGE$_2$ release is enhanced in response to BK-induced COX-2 expression

COX-2 catalyzes the rate-limiting step of arachidonic acid conversion to prostaglandins, including PGE$_2$. PGE$_2$ is the major biologically active product of the COX-2 pathway (20), and increases cell proliferation and motility. We determined whether PGE$_2$ is released in conjunction with BK-stimulated COX-2 expression. PCI-37A cells were cultured in the presence of BK (10 nM), and culture supernatants were collected at various time points up to 16 h. As shown in Fig. 2, there was a time-dependent accumulation of PGE$_2$ that became significant after 1 h ($P < 0.05$), peaked at 4-fold higher than baseline at 4 h, and declined after 4 h of treatment. These results were observed in two replicate experiments, and show that BK activation of COX-2 in HNSCC is accompanied by PGE$_2$ release.

At 8 and 16 h, there is still an elevation of COX-2 protein as seen in Fig. 1B, but PGE2 levels released into the culture medium were at basal values. This could be due to low sensitivity of the ELISA assay, internalization of PGE2 by binding to its receptors (since HNSCC cells respond to PGE2 [8]), or lack or PGE2 precursor at the later time points. In two experiments using 1 μM BK, only slight increases in PGE2 release (10-12 pg/ml) were observed over a 16 h time period, in agreement with the biphasic responses we observed in COX-2 expression (data not shown).

BK induces MAPK phosphorylation

BK has previously been shown to mediate EGFR transactivation (3, 8), which can result in phosphorylation of MAPK. Under similar conditions that result in COX-2 induction in HNSCC cells, BK also caused activation of MAPK in a time- and concentration-dependent manner. We found that phospho-MAPK was increased significantly above baseline and was maximal at a concentration of 10 nM BK (Fig. 3A); the increase occurred within 5-10 min of BK addition in PCI-37A cells ($P < 0.05$; Fig. 3B) and declined over 1-2 h. Thus maximal activation of MAPK occurred at the same concentration of BK as the induction of COX-2, and appearance of phospho-MAPK preceded COX-2 induction. Results are from three independent experiments. We did not observe a biphasic response in phospho- MAPK

induction, which may not occur because phosphorylation of MAPK occurs rapidly, before desensitization induced by higher concentrations of BK is complete. MAPK activation is necessary for COX-2 induction (see Fig. 5C), but may not be sufficient, since it is not diminished at concentrations of BK that show weak ability to induce COX-2 mRNA and protein. In our previous study of COX-2 induction by hepatocyte growth factor (22), we found both MAPK and p38 were required, and participated in phosphorylating multiple transcription factors that bind the COX-2 promoter, most likely at more than one phosphorylation site. Inhibition of either MAPK or p38 prevented COX-2 induction (22). It is possible that biphasic responses to BK are present in other steps that are also needed for COX-2 induction in HNSCC cells.

BK mediates signaling through B2R

BK is an agonist for B2R and signals primarily through this receptor. Although BK does not have affinity for B1R, it can be metabolized by kinin to des-Arg[9]-bradykinin which activates B1R (23). Moreover, the B1R and B2R can exhibit cross-talk with each other at the level of heterotrimeric G-proteins (13). To determine the receptor subtype involved in BK signaling in HNSCC, the cells were pretreated with increasing concentrations of the B2R antagonist HOE140, which is highly selective for the B2R with a Ki less than 0.5 nM amd virtually no affinity for the B1R (24) or the highly selective B1R antagonist Lys (Des-Arg[9]-Leu[8]) BK, which has a Ki for B1R in the nM range and over a 10,000-fold lower affinity for the B2R (25), followed by treatment with BK. The B2R antagonist, but not the B1R antagonist, inhibited BK-induced EGFR and MAPK activation, and COX-2 induction (Fig. 4). Fig. 4A depicts EGFR tyrosine phosphorylation in HNSCC after treatment with BK, assessed after immunoprecipitation with an anti-EGFR antibody. Tyrosine phosphorylation of EGFR was enhanced 10-fold by treatment with 10 nM BK. BK-activated EGFR tyrosine phosphorylation was inhibited 70% by 10 μM HOE 140. However, phosphorylation of EGFR was not appreciably inhibited by pretreatment with concentrations of B1R antagonist up to 10 μM. Likewise, the B2R antagonist, but not B1R antagonist, inhibited MAPK activation (Fig. 4B). An 80% reduction in p-MAPK was observed with HOE140 ($P < 0.01$), while the B1R antagonist had no effect (n.s.). The effect of BK-induced COX-2 protein expression was also significantly reduced by HOE140, but not B1R antagonist. BK-induced COX-2 levels measured are below baseline, p=0.002, when cell are pre-treated with HOE140 at 0.1 μM or more, but B1R antagonist shows no effect (p=0.48 with B1R antagonist from 1 -50 μM, Fig. 4C). These results support the role of the B2R, and not the B1R, in mediating COX-2 induction after treatment with BK.

To confirm that COX-2 protein expression and MAPK activation were not regulated by B1R, we examined p-MAPK and COX-2 protein levels following treatment of PCI-37A cells with increasing concentrations of B1R-agonist (Des-Arg[9]-BK). As shown in Fig. 4D, the B1R-agonist had no effect on either p-MAPK activation or COX-2 expression in PCI-37A cells after B1R-agonist (Des-Arg[9]-BK) treatment.

EGFR and MAPK are required for COX-2 induction by BK

Since BK activates the EGFR pathway, we next tested the contribution of this pathway to COX-2 induction. We pretreated PCI-37A cells with EGFR tyrosine kinase inhibitor tyrosine gefitinib for 30 min before addition of 10 nM BK. We found that the BK-induced COX-2 was significantly abrogated in the presence of 1 μM gefitinib (71.4% inhibition, $P < 0.05$, Fig. 5A). EGFR also appeared to contribute to the baseline expression of COX-2 since either agent alone decreased the basal COX-2 protein levels.

BK is known to activate EGFR by a src-dependent release of EGFR ligand in HNSCC (8). We confirmed that under the conditions used for EGFR activation and COX-2 induction in

HNSCC cells, the effect of BK on EGFR phosphorylation was inhibited by blocking the external EGFR ligand binding site with the antibody C225 (Fig. 5B, left panel). BK-induced activation of PY1068-EGFR was blocked over 90% by C225. Published data from our laboratory has shown the EGFR ligand most likely responsible for mediating BK effects is TGFα (8). The EGFR inhibitor gefitinib also completely blocked formation of PY1068-EGFR (Fig. 5B, right panel), suggesting the effect is due to autophosphorylation of EGFR, rather than to a different kinase. This is consistent with a response mediated by EGFR ligand. Since BK activates the src-EGFR pathway, we also tested the contribution of this pathway to COX-2 induction (Fig. 5A). We found that BK-induced increase in COX-2 was also abrogated by pretreatment with the src inhibitor AZD0530 (81% inhibition, $P < 0.05$). These results suggest that both src and EGFR are involved in COX-2 induction by BK. Inhibition of src alone, or inhibition of EGFR alone was sufficient to abrogate COX-2 induction, suggesting that these two molecules act in the same pathway rather than through independent pathways, to induce COX-2. We previously reported that src is activated by GPCR ligands and is responsible for the activation of proteases that cleave EGFR pro-ligands to their active forms in SCCHN, providing a mechanism for EGFR activation (17).

Since MAPK is downstream of EGFR activation, we explored whether MAPK activation is required for BK-induced COX-2 expression. Two MEK inhibitors, PD98059 and U0126, were used, both of which block phosphorylation of MAPK by MEK. We measured the effect of PD98059 and U0126 on BK-induced expression of COX-2 (Fig. 5C). Pretreatment of PCI-37A cells with PD98059 (1~50 μM) or U0126 (1~50 μM) for 30 min before addition of 10 nM BK caused a significant reduction of BK-induced COX-2 expression in a concentration-dependent manner. When cells were pre-treated with 1 μM PD98059, BK-induced COX-2 expression was inhibited by 85%; while in cells pre-treated with 1 or 10 μM U0126, BK-induced COX-2 expression was also reduced 85% ($P < 0.05$, Fig. 5C). These results confirm that MAPK activation is upstream of BK-induced COX-2 expression.

B2R is over-expressed in HNSCC tumors

Since B2R was found to mediate signaling by BK in HNSCC cells, we examined expression of B2R in HNSCC cell lines and found that B2R was expressed in all three HNSCC tumor cell lines tested, 1483, UM-22B and PCI-37A, as well as in an immortalized cell line derived from normal mucosa of the esophagus, HET1A (Fig. 6A). This is in accordance with previous reports that B2R is ubiquitously present even in normal tissue (26). The level of B2R protein was found to be 2.2, 1.6, 2.6 times higher when normalized for β-actin in the 1483, UM-22B and PCI-37A tumorigenic cells respectively, compared to the HET1A cells. This suggests that B2R is over-expressed in HNSCC tumors.

To determine whether B2R levels are modulated in HNSCC tumors, we compared the proteins levels of B2R in lysates of six HNSCC primary tumors and corresponding normal mucosa from the same patients. Immunoblot analysis revealed that B2R expression was higher on average in tumors by 2.8-fold as compared to normal mucosa (Fig. 6B). B2R levels in paired tumor tissue and normal mucosal tissue from 43 patients were also compared by immunohistochemical staining. The clinical and pathologic characteristics of 43 patients whose HNSCC samples were analyzed for B2R staining are shown in Table 1. B2R staining was found primarily in the tumor cells and was undetectable in the stroma (Fig. 6C). Low levels of B2R staining were observed in normal tissue. Wilcoxon signed rank analysis of IHC mean staining intensity values revealed that B2R levels were 3-fold higher in tumor tissue compared to normal control tissue and the difference was statistically significant (Fig. 6C, P=0.045). B1R was detected by IHC in only a small percentage of tumor and normal tissue, and did not show statistical differences, suggesting that the B1R is not significantly expressed in HNSCC (data not shown). These results show that B2R, but

not B1R, is over-expressed in head and neck tumor, compared to control normal tissue from the same patient, and confirms results seen in cell lines.

B2R levels in HNSCC do not correlate with clinical characteristics

Many tumorigenic signaling molecules such as EGFR are upregulated upon disease progression and an increase in their levels correlates with poor prognosis and decreased survival (27). We investigated the possibility that B2R levels (measured as staining intensity by IHC) in HNSCC may correlate with patient survival or with tumor stage. However there was no significant correlation between median survival or time to progression and B2R intensity (Logrank P= 0.88) or B2R weighted intensity (Logrank P=0.48). There was also no correlation between B2R intensity and T stage (p=0.14), N stage (p=0.8) of the tumor, or of smoking status (p = 0.66) of the patient. These data suggest that B2R up-regulation is not restricted to tumors from patients with tobacco exposure or with HNSCC disease progression. How early in the course of HNSCC tumor development B2R over-expression occurs remains to be determined.

Similarly, there was also no correlation between patient survival and B1R intensity (Logrank $P = 0.1$) or B1R weighted intensity (Logrank $P = 0.24$). Thus B1R is not only poorly expressed in HNSCC, but also its expression level does not correlate with disease prognosis.

DISCUSSION

Our findings that B2R is over-expressed in HNSCC and has important biological functions including induction of the pro-tumorigenic enzyme COX-2 support the involvement of this GPCR in HNSCC tumorigenesis. Kinins such as BK and kallidin, as well as the BK receptors, have been previously implicated in inflammation and hyperalgesia, and recently a role for these receptors in tumorigenesis has been identified (26). B2R knockout mice showed decreased growth of tumor xenografts due to reduced angiogenesis (28). It is thought that B2Rs are expressed constitutively by a variety of cells while B1Rs are induced in response to inflammation and injury. In contrast, our study revealed insignificant levels of B1R in HNSCC tumors, whereas B2R was over-expressed in HNSCC. Similar to our findings, B2R levels have been found to be over-expressed in human gliomas, where they increase with increasing tumor grade (10). However, in our study, there was no correlation between the level of B2R expression and HNSCC tumor stage or survival, suggesting that multiple pathways besides B2 signaling contribute to HNSCC tumorigenesis. In our study, B2R was expressed exclusively in HNSCC tumor cells and was not detected in the stroma. This is in contrast to esophageal carcinoma where giant cells and mast cells infiltrating the tumor expressed B2R (29). Also, we did not observe any microvessel staining of B2R, although B2Rs have been implicated in angiogenesis (28) and increase in vascular permeability. Supporting our finding of B2R expression in tumor cells of HNSCC patients, we found that B2R was expressed and mediated tumorigenic signaling in cultured HNSCC cell lines. Thus the role of B2R in tumorigenesis appears to vary depending on the tumor type; in HNSCC, its role appears to be restricted to tumor cells.

COX-2 is thought to be responsible in various inflammation and tumorgenesis. COX-2 is an important target for chemoprevention in HNSCC and other tumors (30). Induction of COX-2 often serves as an amplification mechanism for proliferative signaling. For example, the product of COX-2, PGE2, itself increases COX-2 levels through its GPCR, generating a positive feedback loop (31). It appears that BK also employs COX-2 to amplify its tumorigenic effect in HNSCC. In this study, we found that treatment of head and neck cancer cells with BK induced subsequent activation of EGFR, MAPK, and expression of COX-2. These findings are consistent with our previous study in HNSCC (8), in which we demonstrated that BK induced EGFR ligand release and activated EGFR downstream

signaling. In this previous report, we also found that MAPK induction by BK was inhibited by a small molecule EGFR tyrosine kinase inhibitor and C225, demonstrating involvement of EGFR in BK-induced MAPK signaling in HNSCC. We also detected some EGFR-independent signaling by BK to MAPK (8), suggesting that there may be additional mechanisms of MAPK activation by BK. However, in the studies reported here, B2R antagonist, EGFR inhibition, and MEK inhibitors all prevented BK-induced COX-2 expression, suggesting that the BK-EGFR-MAPK-signaling axis is upstream of COX-2. It is possible that other molecules besides EGFR participate in BK induction of MAPK, but probably not in signaling complexes that activate COX-2. These results suggest that the EGFR/MAPK signaling pathway is required for the induction of COX-2 caused by BK. In addition, there is no effect on activation of MAPK and expression of COX-2 when HNSCC cells were treated with B1R agonist. This further supports that the involvement of B2R, but not B1R, in BK signaling in HNSCC.

We also found that the autophosphorylation of EGFR site Y1068 in response to BK is most likely mediated through extracellular ligand release since it was inhibited by the EGFR antibody C225, which blocks the external ligand binding site. Previous studies from our group have shown that BK-mediated regulation of total EGFR phosphorylation is mediated through Src Family Kinase-dependent activation of a metalloproteinase, tumor necrosis-factor alpha converting enzyme (TACE), which releases TGF-α to activate EGFR (8). Therefore it is very likely that BK-mediated EGFR autophosphorylation also involves TACE activation and TGF-α release. Phosphorylation of EGFR at different sites leads to differential recruitment of signaling molecules. For example, phosphorylation of EGFR at Y1068 leads to recruitment of a shc/Grb/SOS complex (32) while phosphorylation at Y845 results in STAT5b activation (33). Previous studies from our group have shown that inhibition of EGFR kinase activity using erlotinib or gefitinib inhibited BK-induced MAPK activation, cell growth and migration of HNSCC (8), suggesting that EGFR autophosphorylation is required for BK function in HNSCC. It is very likely that abrogation of EGFR phosphorylation will also inhibit effects of BK on growth, similar to reports on other GPCRs in cancer cells (34).

The signaling routes linking GPCRs to MAPK often involve EGFR tyrosine kinases phosphorylation. We show that a similar cross-talk involving activation of the EGFR/MAPK pathway by BK results in increased levels of COX-2. Over-expression of COX-2 often acts as an amplification mechanism for proliferation. For example, p60-v-src transformation of 3T3 fibroblasts results in high COX-2 levels (35). EGFR mediates expression of COX-2 in response to tobacco smoke exposure in oral cells (36). COX-2 is an important target for chemoprevention in HNSCC and other tumors (30). Our study also demonstrates B2R overexpression in HNSCC. B2R is known to be involved in autocrine or paracrine mechanisms that assist tumor growth, vascular permeability and metastasis (37), which might relate to cancer survival. However, our data show no association between B2R expression and survival or tumor stage in 43 HNSCC patients. Larger sample sizes with a higher power to determine the relationship between HNSCC patient survival, tumor stage and B2R overexpression may be necessary to show an association. Alternatively, the level of EGFR expression, which is a major mediator of BK effects, may be a more important factor in patient survival.

Previous studies performed in HNSCC, targeting molecules in the above pathway in combination, have shown synergistic anti-tumor effects. In particular, inhibition of EGFR and COX-2 (19) and inhibition of BK receptor and EGFR (8) have shown increased efficacy in HNSCC. Our study supports the potential for targeting B2R antagonists in combination with EGFR, MEK or COX-2 inhibitors. Such combination therapies might reduce the dose required for each drug, thus reducing toxicity and enhancing efficacy.

BK receptor antagonists are already in clinical trials for a number of disorders. The B2R antagonist HOE140 is under clinical trial for the treatment of angioedema (Clinicaltrials.gov Identifier: NCT00097695; currently in Phase III studies by Jerini Pharma), osteoarthritis (Clinicaltrials.gov identifier: NCT00303056), and has also shown improvement in pulmonary function in a clinical trial for asthma (38). Our finding that B2R mediates tumorigenic pathways in HNSCC provides a rationale for additional preclinical studies with B2R antagonists in HNSCC which could lead to clinical testing for cancer therapy. It is not known if a therapeutic approach using B2R antagonists would be superior to COX-2 inhibition, would be additive with COX-2 or EGFR inhibition, or would have fewer toxicities than COX-2 inhibitors. Because so many GPCRs can activate EGFR via Src family kinases (8), a Src family kinase inhibitor such as dasatinib may be more beneficial than blocking only one GPCR type, such as B2R, unless a tumor demonstrated particular dependence on the B2R pathway.

MATERIAL AND METHODS

Materials

Cell culture reagents DMEM, BME and FBS were obtained from Invitrogen (Carlsbad, CA). B1 and B2 receptor antibodies and their blocking peptides were purchased from SantaCruz Biotechnology (SantaCruz, CA). PY1068-EGFR, Phospho-p42/p44-MAPK and p42/p44-MAPK antibodies and MEK inhibitors, PD98059 and U126, were from Cell Signaling Technology (Beverly, MA). EGFR antibody and anti-phosphotyrosine antibody (PY20) were purchased from BD Biosciences (San Jose, CA). COX-2 antibody was from Cayman Chemical Company (Ann Arbor, MI) and beta-actin antibody was from Chemicon (Temecula, CA) and Abcam (Cambridge, MA). Antibodies to total and phospho-MAPK were from Cell Signaling (catalogue number 9101 and 9102). Gefitinib was a gift from Astrazeneca (Wilmington, DE) and the EGFR antibody C225 (erbitux) was a gift from Imclone (New York, NY). B1R antagonist Lys (Des-Arg[9]-Leu[8])-BK and B2R antagonist HOE140 were purchased from Sigma (St. Louis, MO) and from Biomol Research Laboratories (Plymouth Meeting, PA), respectively. Gefitinib, erlotinib, PD98059 and U126 were dissolved in DMSO and stored in aliquots at -20 °C. The BK antagonist CU201 was a kind gift from Dr. Daniel Chan (Denver, Colorado), the peptides EGF, BK and the B1R agonist Lys (Lys-Des-Arg[9])-BK were purchased from Invitrogen, Bachem (Torrance, CA), and from Sigma respectively, dissolved in water and stored in aliquots at -80°C. PGE_2 enzyme immunoassay kit was purchased from Cayman Chemical (Ann Arbor, MI).

Cell culture

PCI-37A (39), 1483 (40), and UM-22B (41) HNSCC cells were cultured in BME (Basal Medium Eagle's) with 1% fetal bovine serum and L-glutamine and serum-deprived using BME for 2 to 3 days, followed by stimulation with BK for experiments. HET-1A (42) is an immortalized human esophageal epithelial cell line. For determination of B2R levels, HET-1A cells, PCI-37A cells, 1483 cells, and UM-22B cells were grown in DMEM+10% FBS.

Immunohistochemistry (IHC)

Paraffin-embedded slides with head and neck tumor tissue and adjacent normal control tissue from 43 HNSCC patients were stained using B1R and B2R antibodies. Kidney slides were used as positive controls for B1R and B2R staining. Blocking peptides were used to confirm the specificity of the antibodies for this application. A standard streptavadin-biotin approach was used to stain the slides after microwave pretreatment for antigen retrieval. The slides were examined microscopically and were scored in a blinded fashion using a semi-quantitative scoring system. The amount of tumor was scored as a percentage of the overall

tumor in the section with positive staining. The intensity of the stain was scored on a scale of 0 to 3, with 0 indicating absent staining and 3 being the highest intensity of staining. An overall staining score was obtained by multiplying the intensity of staining by the percentage of tissue showing that level of intensity. These values for tumor and normal tissue were then compared using the Wilcoxon signed rank test by Graphpad Instat statistical analysis program. P values less than 0.05 were considered statistically significant.

Immunoblotting

Immunoblotting was used to determine the protein levels of EGFR, phosphorylated EGFR, phosphorylated MAPK, and COX-2. Subsequent to treatment with inhibitors and agonists, HNSCC cells were lysed in ice-cold radioimmunoprecipitation assay (RIPA) buffer containing protease inhibitor cocktail tablet (Roche, Indianapolis, IN) and phosphatase inhibitors (Na3VO4 and NaF). Proteins were resolved by SDS-PAGE using 6% Tris-glycine gels for EGFR and 10% gels for COX-2, transferred onto nitrocellulose membranes, and blocked with 5% BSA (to measure phosphorylated proteins) or 5% milk (to measure total protein levels). Primary antibody diluted in blocking solution was added and incubated overnight. Horseradish peroxidase-conjugated secondary antibody was then used, followed by chemiluminescent detection using the ECL kit (Amersham). In some experiments, total phosphorylation of EGFR was determined by immunoprecipation and immunoblotting with an antibody to phospho-tyrosine. EGFR protein was first immunoprecipitated with 1.2 μg of anti-EGFR antibody and resolved on an 8% SDS-PAGE gel. Following transfer to nitrocellulose membrane, the membrane was blocked in 5% Blotto solution and probed with 1:1000 dilution of anti-phosphotyrosine (PY20) antibody.

Protein levels of B2R were compared between tumor and normal tissue for each head and neck cancer patient, by immunoblotting. For this experiment, tumor and normal tissue were obtained from six head and neck cancer patients. The tissue lysates were resolved by SDS-PAGE, probed using B1R and B2R antibodies (dilution of 1:200), and beta-actin antibody (dilution of 1:10,000). Densitometric analysis of the blots was performed using the ScionImage program, which yielded numerical values that were plotted to generate graphs. The same immunoblotting methodology was followed to determine the levels of these receptors in lysates of head and neck cell lines HET-1A, 1483, PCI-37A and UM-22B.

Specificity of the B2R antibody was confirmed by peptide competition. For this experiment, B2R antibody was pre-incubated with a five-fold excess of B2R blocking peptide. This mixture was added to a blot containing cell lysate proteins and incubated overnight; another identical blot was incubated in parallel with B2R antibody alone. Absence of the 75 kD B2R band in the blot incubated with blocking peptide plus antibody, was used to demonstrate the specificity of the antibody for B2R.

Enzyme-Linked Immunosorbent Assay (ELISA)

For the detection of PGE_2 release, PCI-37A cells were grown in 60 mm × 60mm dishes to 75% confluence and then serum deprived for 48 hours. The culture medium was replaced with 3 ml of serum free fresh BME, and BK (10 nM) was added. After treatment for the indicated time period, the supernatants were harvested and stored at -80°C until subsequent assay of PGE_2 release. The same cells were also cultured in a similar manner to examine COX-2 protein expression by immunoblot. 50 μl of supernatant from each sample was used for analysis PGE_2 using a Prostaglandin E2 EIA kit (Cayman Chemicals) and following the manufacturer's instruction. Briefly, 50 μl of the medium, along with a serial dilution of PGE_2 standard samples, was mixed with appropriate amounts the AchE Tracer and PGE_2 antiserum, and incubated at 4°C on a shaker for 18 h. After the wells were emptied and rinsed with wash buffer, 200 μl of Ellman's reagent containing substrate for

acetylcholinesterase was added. The enzyme reaction was carried out on a slow shaker at room temperature for 1.5 h. The absorbance at 405 nm was determined using a Wallac Victor[2] 1420 Multilabel Counter (PerkinElmer). Assays were performed in duplicate and are expressed as picograms per milliliter.

Statistical analysis

Values shown represent means ± SD. Statistical analysis for biochemical assays was performed by Student t test with a p value of less than 0.05 being considered statistically significant. Statistical determinations for immunohistochemical staining results were carried out by Wilcoxon signed rank test using Graphpad Instat statistical analysis program to evaluate the staining score between tumor and normal tissue. P values less than 0.05 were considered statistically significant.

Supplementary Material

Refer to Web version on PubMed Central for supplementary material.

Acknowledgments

Abbreviations

|	
BK	bradykinin
COX-2	cyclo-oxygenase-2
EGFR	epidermal growth factor receptor
HNSCC	squamous cell carcinoma of the head and neck
MAPK (ERK1/2)	mitogen-activated protein kinase
MEK	mitogen activated protein kinase kinase

References

1. Darmoul D, Gratio V, Devaud H, Laburthe M. Protease-activated receptor 2 in colon cancer: trypsin-induced MAPK phosphorylation and cell proliferation are mediated by epidermal growth factor receptor transactivation. J Biol Chem. 2004; 279(20):20927–34. [PubMed: 15010475]

2. Fischer OM, Hart S, Gschwind A, Ullrich A. EGFR signal transactivation in cancer cells. Biochem Soc Trans. 2003; 31(Pt 6):1203–8. [PubMed: 14641026]

3. Gschwind A, Prenzel N, Ullrich A. Lysophosphatidic acid-induced squamous cell carcinoma cell proliferation and motility involves epidermal growth factor receptor signal transactivation. Cancer Res. 2002; 62(21):6329–36. [PubMed: 12414665]

4. Raj GV, Barki-Harrington L, Kue PF, Daaka Y. Guanosine phosphate binding protein coupled receptors in prostate cancer: a review. J Urol. 2002; 167(3):1458–63. [PubMed: 11832770]

5. Venkatakrishnan G, Salgia R, Groopman JE. Chemokine receptors CXCR-1/2 activate mitogen-activated protein kinase via the epidermal growth factor receptor in ovarian cancer cells. J Biol Chem. 2000; 275(10):6868–75. [PubMed: 10702246]

6. Li S, Huang S, Peng SB. Overexpression of G protein-coupled receptors in cancer cells: involvement in tumor progression. Int J Oncol. 2005; 27(5):1329–39. [PubMed: 16211229]

7. Krysan K, Reckamp KL, Dalwadi H, Sharma S, Rozengurt E, Dohadwala M, et al. Prostaglandin E2 activates mitogen-activated protein kinase/Erk pathway signaling and cell proliferation in non-small

cell lung cancer cells in an epidermal growth factor receptor-independent manner. Cancer Res. 2005; 65(14):6275–81. [PubMed: 16024629]

8. Thomas SM, Bhola NE, Zhang Q, Contrucci SC, Wentzel AL, Freilino ML, et al. Cross-talk between G protein-coupled receptor and epidermal growth factor receptor signaling pathways contributes to growth and invasion of head and neck squamous cell carcinoma. Cancer Res. 2006; 66(24):11831–9. [PubMed: 17178880]

9. Taub JS, Guo R, Leeb-Lundberg LM, Madden JF, Daaka Y. Bradykinin receptor subtype 1 expression and function in prostate cancer. Cancer Res. 2003; 63(9):2037–41. [PubMed: 12727816]

10. Zhao Y, Xue Y, Liu Y, Fu W, Jiang N, An P, et al. Study of correlation between expression of bradykinin B2 receptor and pathological grade in human gliomas. Br J Neurosurg. 2005; 19(4): 322–6. [PubMed: 16455538]

11. Wu J, Akaike T, Hayashida K, Miyamoto Y, Nakagawa T, Miyakawa K, et al. Identification of bradykinin receptors in clinical cancer specimens and murine tumor tissues. Int J Cancer. 2002; 98(1):29–35. [PubMed: 11857381]

12. Exton JH. Phospholipase D-structure, regulation and function. Rev Physiol Biochem Pharmacol. 2002; 144:1–94. [PubMed: 11987824]

13. Barki-Harrington L, Bookout AL, Wang G, Lamb ME, Leeb-Lundberg LM, Daaka Y. Requirement for direct cross-talk between B1 and B2 kinin receptors for the proliferation of androgen-insensitive prostate cancer PC3 cells. Biochem J. 2003; 371(Pt 2):581–7. [PubMed: 12534343]

14. Greco S, Muscella A, Elia MG, Romano S, Storelli C. Marsigliante S Mitogenic signalling by B2 bradykinin receptor in epithelial breast cells. J Cell Physiol. 2004; 201(1):84–96. [PubMed: 15281091]

15. Chen BC, Yu CC, Lei HC, Chang MS, Hsu MJ, Huang CL, et al. Bradykinin B2 receptor mediates NF-kappaB activation and cyclooxygenase-2 expression via the Ras/Raf-1/ERK pathway in human airway epithelial cells. J Immunol. 2004; 173(8):5219–28. [PubMed: 15470067]

16. Chan G, Boyle JO, Yang EK, Zhang F, Sacks PG, Shah JP, et al. Cyclooxygenase-2 expression is up-regulated in squamous cell carcinoma of the head and neck. Cancer Res. 1999; 59(5):991–4. [PubMed: 10070952]

17. Zhang X, Chen ZG, Choe MS, Lin Y, Sun SY, Wieand HS, et al. Tumor growth inhibition by simultaneously blocking epidermal growth factor receptor and cyclooxygenase-2 in a xenograft model. Clin Cancer Res. 2005; 11(17):6261–9. [PubMed: 16144930]

18. Vane JR, Bakhle YS, Botting RM. Cyclooxygenases 1 and 2. Annu Rev Pharmacol Toxicol. 1998; 38:97–120. [PubMed: 9597150]

19. Choe MS, Zhang X, Shin HJ, Shin DM, Chen ZG. Interaction between epidermal growth factor receptor- and cyclooxygenase 2-mediated pathways and its implications for the chemoprevention of head and neck cancer. Mol Cancer Ther. 2005; 4(9):1448–55. [PubMed: 16170038]

20. Yu H, Carretero OA, Juncos LA, Garvin JL. Biphasic effect of bradykinin on rabbit afferent arterioles. Hypertension. 1998; 32:287–92. [PubMed: 9719056]

21. Bawolak MT, Gera L, Morissette G, Stewart JM, Marceau F. B-9972 is an inactivation-resistant agonist of the bradykinin B2 receptor derived from the peptide antagonist B-9430. J. Pharmacol Exp Therapeut. 2007; 323(2):534–46.

22. Siegfried JM, Gubish CT, Rothstein ME, Queiroz de Oliveira PE, Stabile LP. Signaling pathways involved in cyclooxygenase-2 induction by hepatocyte growth factor. Mol Pharmacol. 2007; 72(3):769–79. [PubMed: 17550984]

23. Simpson PB, Woollacott AJ, Hill RG, Seabrook GR. Functional characterization of bradykinin analogues on recombinant human bradykinin B(1) and B(2) receptors. Eur J Pharmacol. 2000; 392(1-2):1–9. [PubMed: 10748265]

24. Hock FJ, Wirth K, Albus U, Linz W, Gerhards HJ, Wiemer G, et al. Hoe 140 a new potent and long acting bradykinin-antagonist: in vitro studies. Br J Pharmacol. 1991; 102(3):769–73. [PubMed: 1364851]

25. Zhang SP, Codd EE. Characterization of bradykinin receptors in human lung fibroblasts using the binding of 3[H] [Des-Arg10, Leu9]kallidin and 3[H]NPC17731. Life Sci. 1998; 62(25):2302–14.

26. Leeb-Lundberg LM, Marceau F, Muller-Esterl W, Pettibone DJ, Zuraw BL. International union of pharmacology. XLV. Classification of the kinin receptor family: from molecular mechanisms to pathophysiological consequences. Pharmacol Rev. 2005; 57(1):27–77. [PubMed: 15734727]

27. Rubin Grandis J, Melhem MF, Gooding WE, Day R, Holst VA, Wagener MM, et al. Levels of TGF-alpha and EGFR protein in head and neck squamous cell carcinoma and patient survival. J Natl Cancer Inst. 1998; 90(11):824–32. [PubMed: 9625170]

28. Ikeda Y, Hayashi I, Kamoshita E, Yamazaki A, Endo H, Ishihara K, et al. Host stromal bradykinin B2 receptor signaling facilitates tumor-associated angiogenesis and tumor growth. Cancer Res. 2004; 64(15):5178–85. [PubMed: 15289322]

29. Dlamini Z, Bhoola K. Esophageal cancer in African blacks of Kwazulu Natal, South Africa: an epidemiological brief. Ethn Dis. 2005; 15(4):786–9. [PubMed: 16259509]

30. Dannenberg AJ, Lippman SM, Mann JR, Subbaramaiah K, DuBois RN. Cyclooxygenase-2 and epidermal growth factor receptor: pharmacologic targets for chemoprevention. J Clin Oncol. 2005; 23(2):254–66. [PubMed: 15637389]

31. Wang D, Buchanan FG, Wang H, Dey SK, DuBois RN. Prostaglandin E2 enhances intestinal adenoma growth via activation of the Ras-mitogen-activated protein kinase cascade. Cancer Res. 2005; 65(5):1822–9. [PubMed: 15753380]

32. Batzer AG, Rotin D, Urena JM, Skolnik EY, Schlessinger J. Hierarchy of binding sites for Grb2 and Shc on the epidermal growth factor receptor. Mol Cell Biol. 1994; 14(8):5192–201. [PubMed: 7518560]

33. Kloth MT, Laughlin KK, Biscardi JS, Boerner JL, Parsons SJ, Silva CM. STAT5b, a Mediator of Synergism between c-Src and the Epidermal Growth Factor Receptor. J Biol Chem. 2003; 278(3): 1671–9. [PubMed: 12429742]

34. Boerner JL, Biscardi JS, Silva CM, Parsons SJ. Transactivating agonists of the EGF receptor require Tyr 845 phosphorylation for induction of DNA synthesis. Mol Carcinog. 2005; 44(4):262–73. [PubMed: 16167350]

35. Han JW, Sadowski H, Young DA, Macara IG. Persistent induction of cyclooxygenase in p60v-src-transformed 3T3 fibroblasts. Proc Natl Acad Sci U S A. 1990; 87(9):3373–7. [PubMed: 2159148]

36. Moraitis D, Du B, De Lorenzo MS, Boyle JO, Weksler BB, Cohen EG, et al. Levels of cyclooxygenase-2 are increased in the oral mucosa of smokers: evidence for the role of epidermal growth factor receptor and its ligands. Cancer Res. 2005; 65(2):664–70. [PubMed: 15695412]

37. Naidoo S, Raidoo DM. Tissue kallikrein and kinin receptor expression in an angiogenic co-culture neuroblastoma model. Metab Brain Dis. 2006; 21(2-3):253–65. [PubMed: 16865540]

38. Akbary AM, Wirth KJ, Scholkens BA. Efficacy and tolerability of Icatibant (Hoe 140) in patients with moderately severe chronic bronchial asthma. Immunopharmacology. 1996; 33(1-3):238–42. [PubMed: 8856156]

39. Heo DS, Snyderman C, Gollin SM, Pan S, Walker E, Deka R, et al. Biology, cytogenetics, and sensitivity to immunological effector cells of new head and neck squamous cell carcinoma lines. Cancer Res. 1989; 49(18):5167–75. [PubMed: 2766286]

40. Sacks PG, Parnes SM, Gallick GE, Mansouri Z, Lichtner R, Satya-Prakash KL, et al. Establishment and characterization of two new squamous cell carcinoma cell lines derived from tumors of the head and neck. Cancer Res. 1988; 48(10):2858–66. [PubMed: 2452013]

41. Grenman R, Carey TE, McClatchey KD, Wagner JG, Pekkola-Heino K, Schwartz DR, et al. In vitro radiation resistance among cell lines established from patients with squamous cell carcinoma of the head and neck. Cancer. 1991; 67(11):2741–7. [PubMed: 2025837]

42. Stoner GD, Kaighn ME, Reddel RR, Resau JH, Bowman D, Naito Z, et al. Establishment and characterization of SV40 T-antigen immortalized human esophageal epithelial cells. Cancer Res. 1991; 51(1):365–71. [PubMed: 1703038]
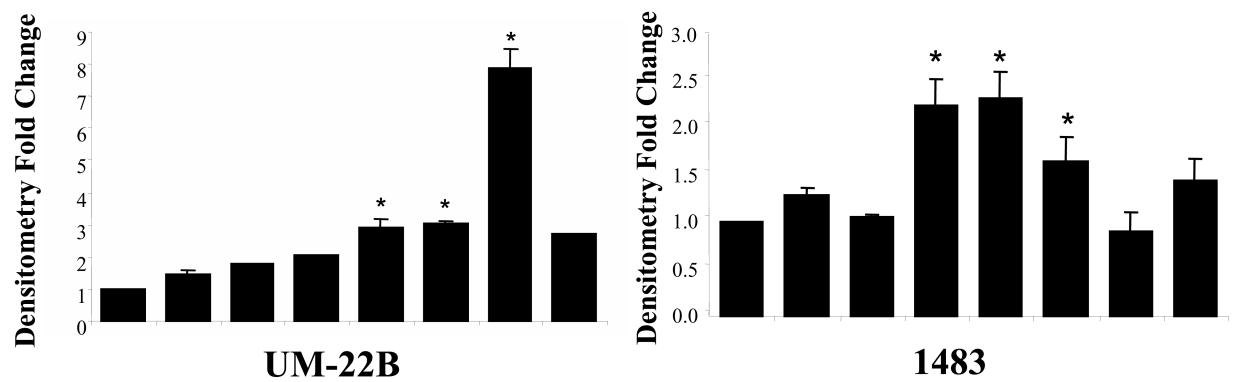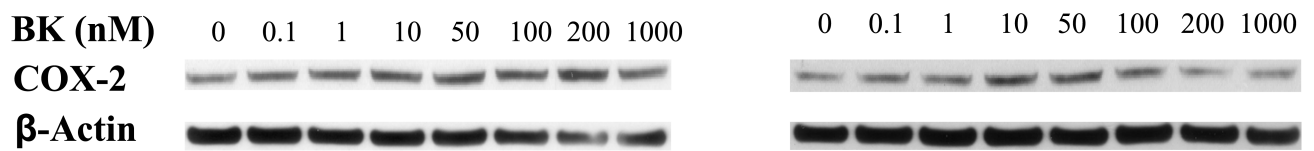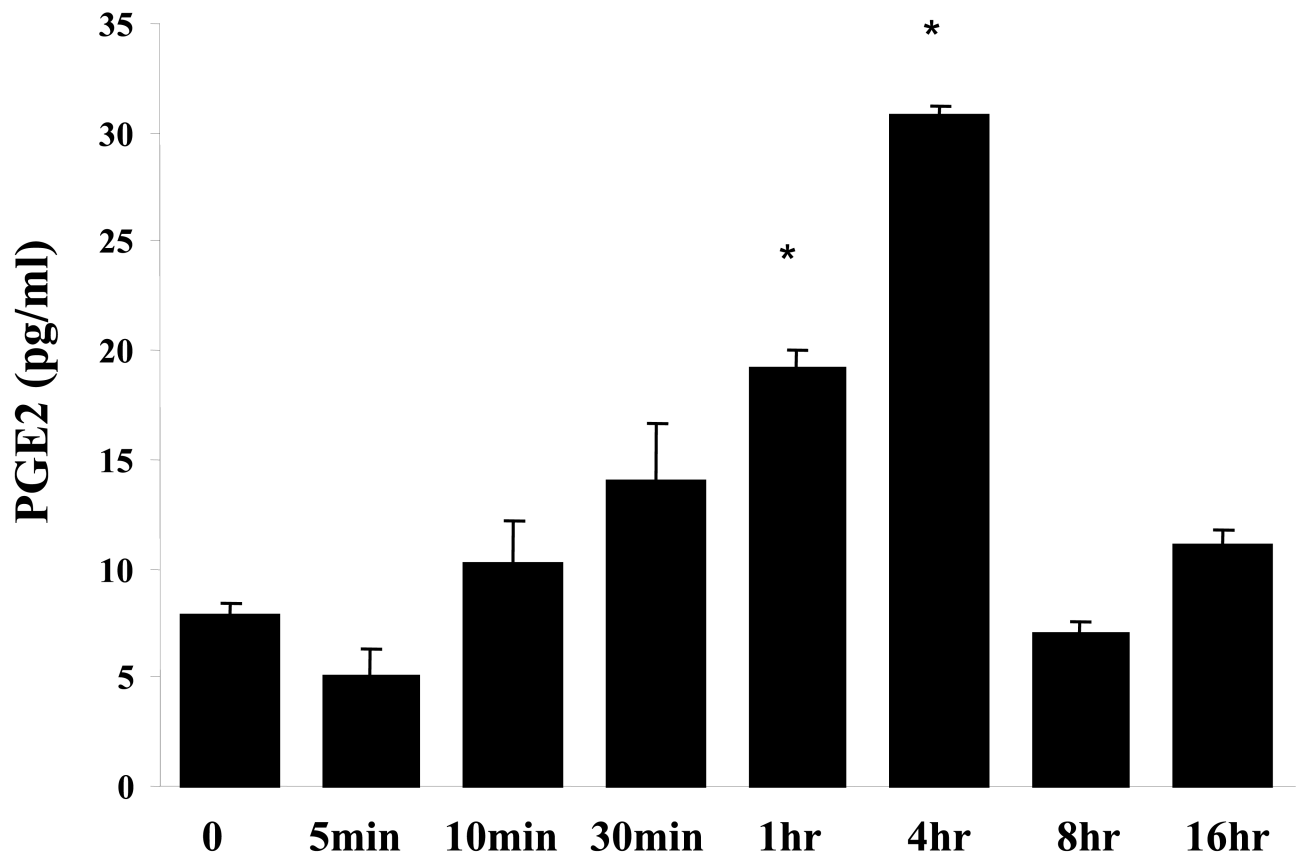
A
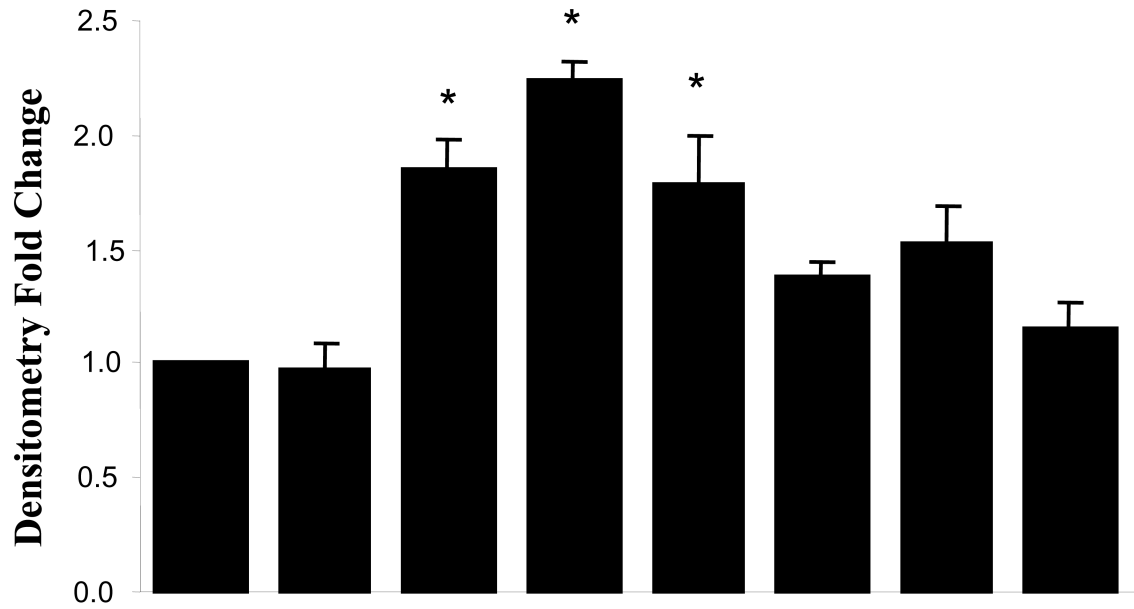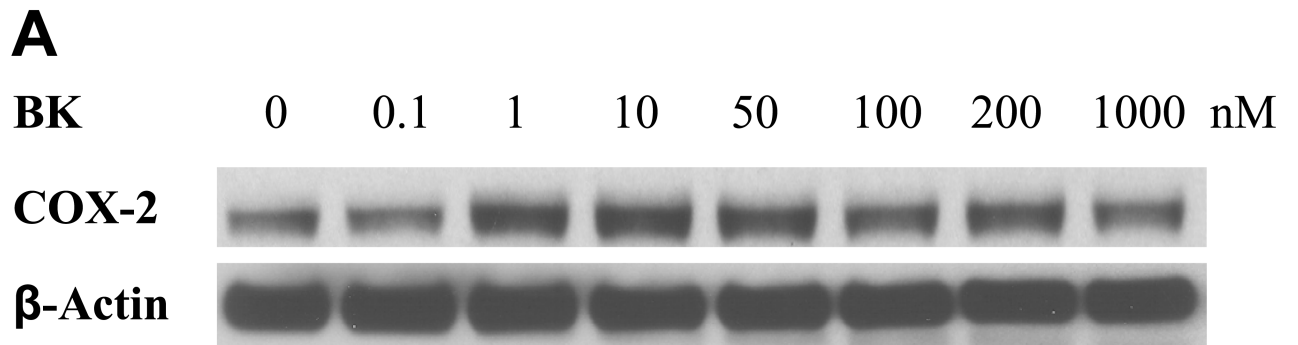
B
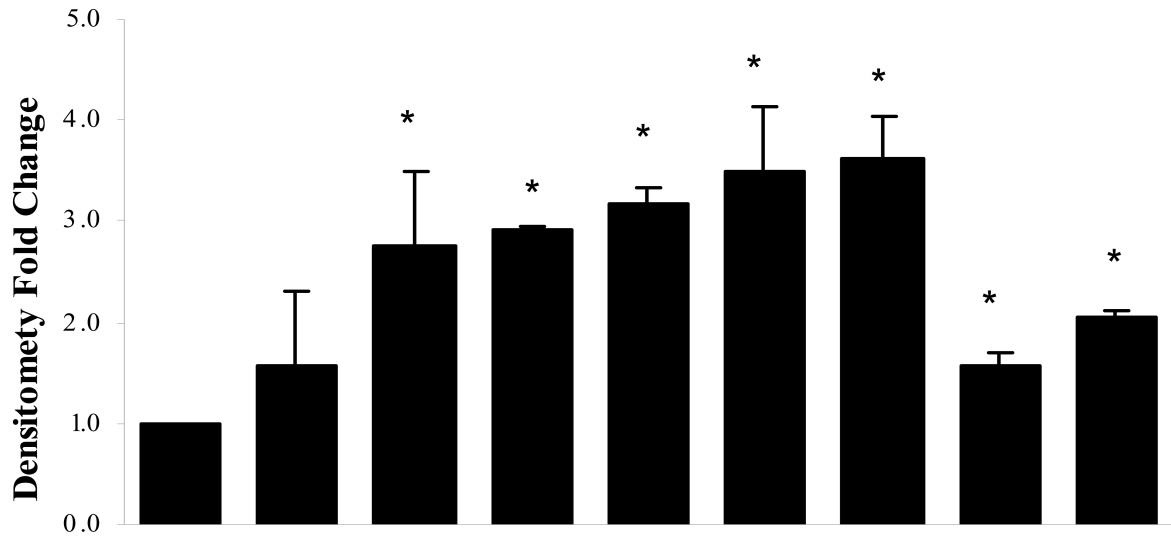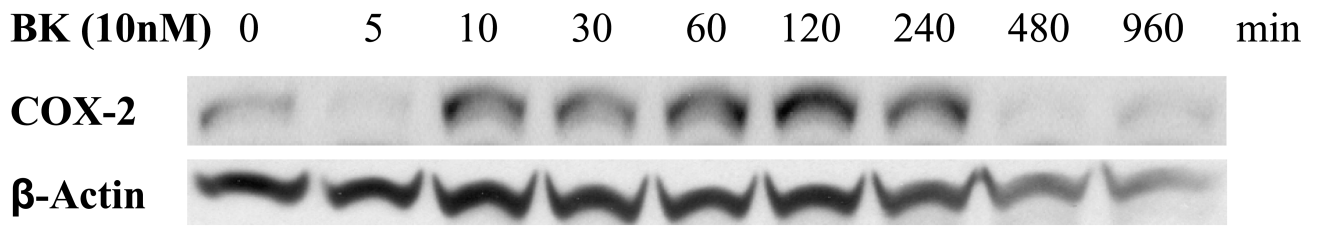
C

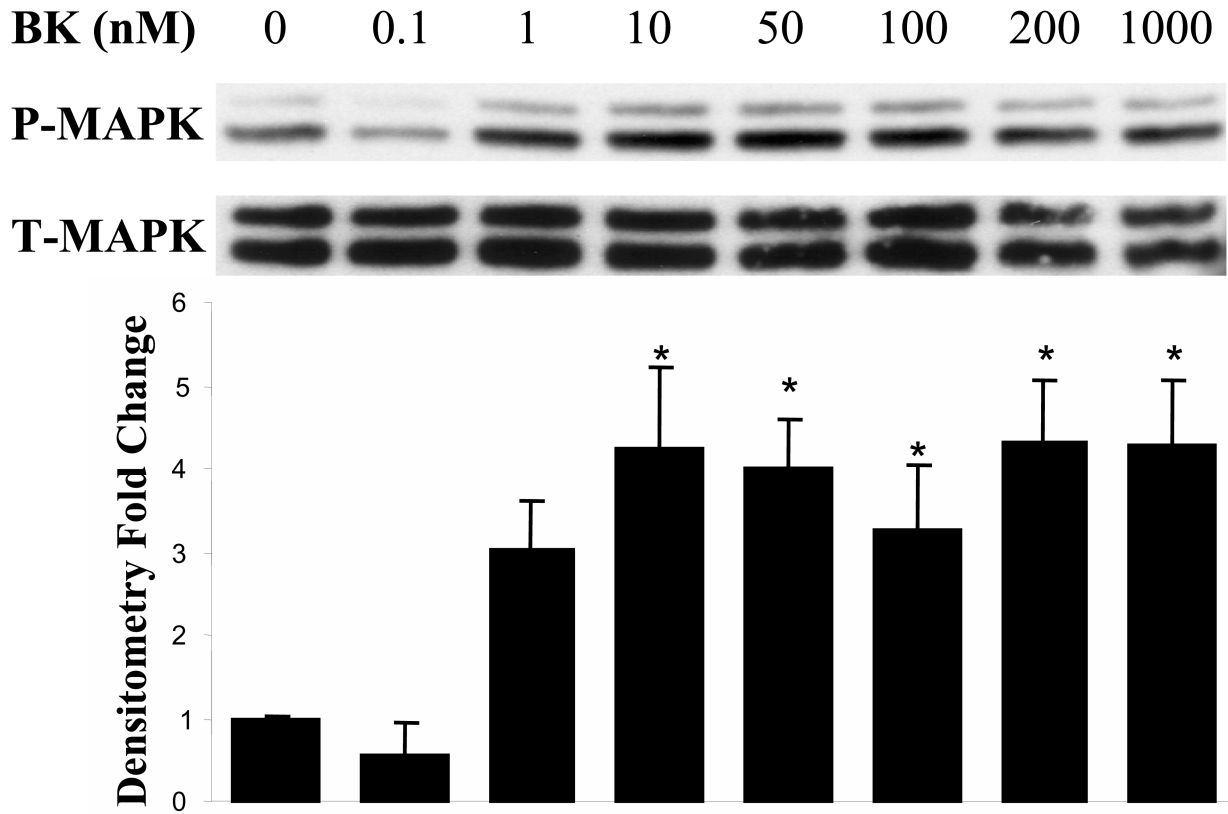**Figure 1. BK-induced COX-2 expression in HNSCC cells**

(A) Dependence of COX-2 expression on BK concentration. PCI-37A cells were serum-starved for 48 h, and then treated with increasing concentrations of BK (0.1 - 1000 nM) for 2 h before harvest. (B) Time course of BK-induced COX-2 expression. PCI-37A cells were serum-starved for 48 h and then treated with10 nM BK for the indicated time intervals. (C) BK-induced COX-2 expression in UM-22B and 1483 HNSCC cell lines. UM-22B and 1483 cells were serum-starved for 48 h, and then treated with increasing concentrations of BK (0.1 - 100 nM) for 2 h before harvest. Whole cell lysates were prepared and then immunoblotted with Abs for COX-2 and β-Actin. Representative immunoblots are shown. The graph presents the fold-change in protein level compared to control as determined by densitometry (cumulative results from three independent experiments) and correlates to the lane shown directly above each bar. Data are expressed as the mean ± SE. Symbol * indicated $P < 0.05$ as compared with the control.

Figure 2. Time course of BK-induced PGE$_2$ release

PCI-37A cells were serum-starved for 48 h and then treated with 10 nM BK for the indicated time intervals at 37° C. The cell culture medium was harvested and 50 µl aliquots were used to measure PGE$_2$ release with an ELISA kit (Cayman Chemicals). Results are means ± SE from three independent experiments. Symbol * indicated $P < 0.05$ as compared with the control.
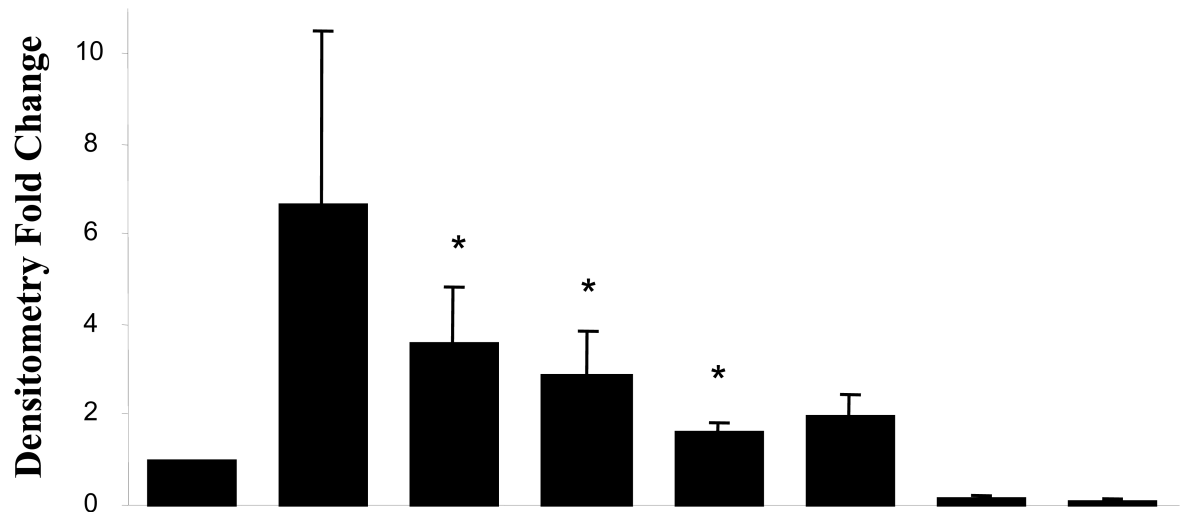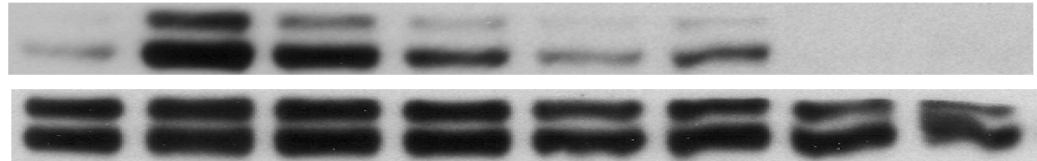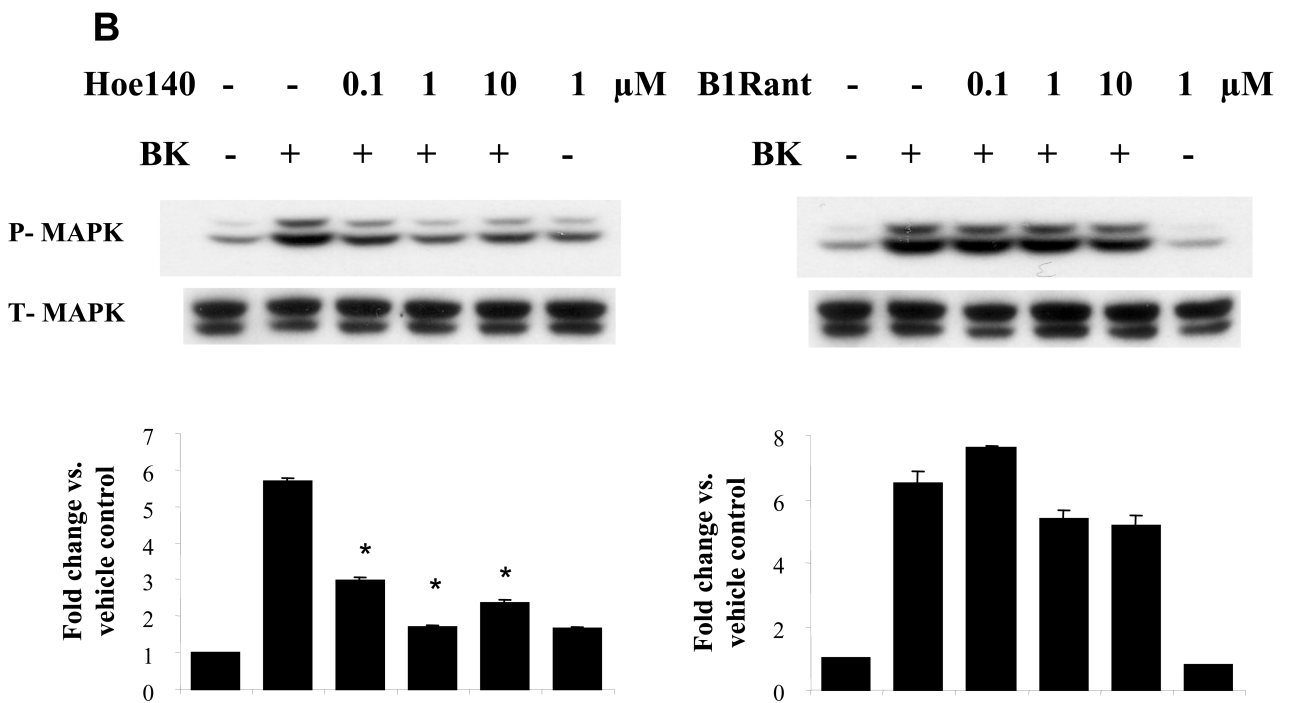
A
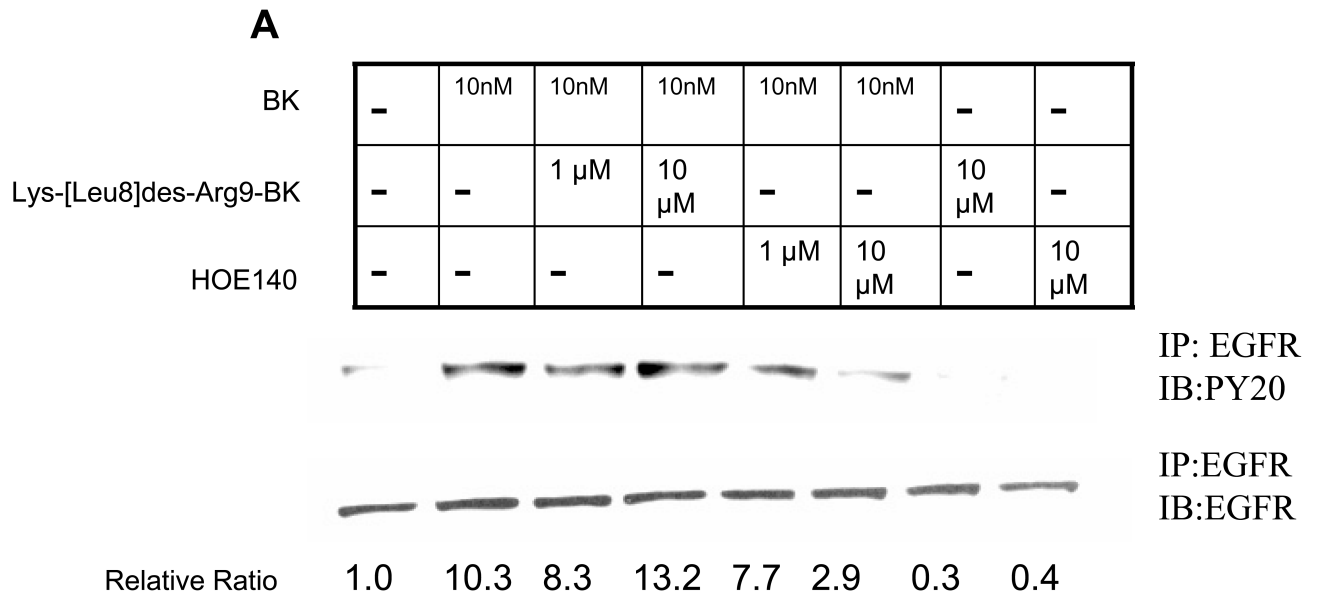
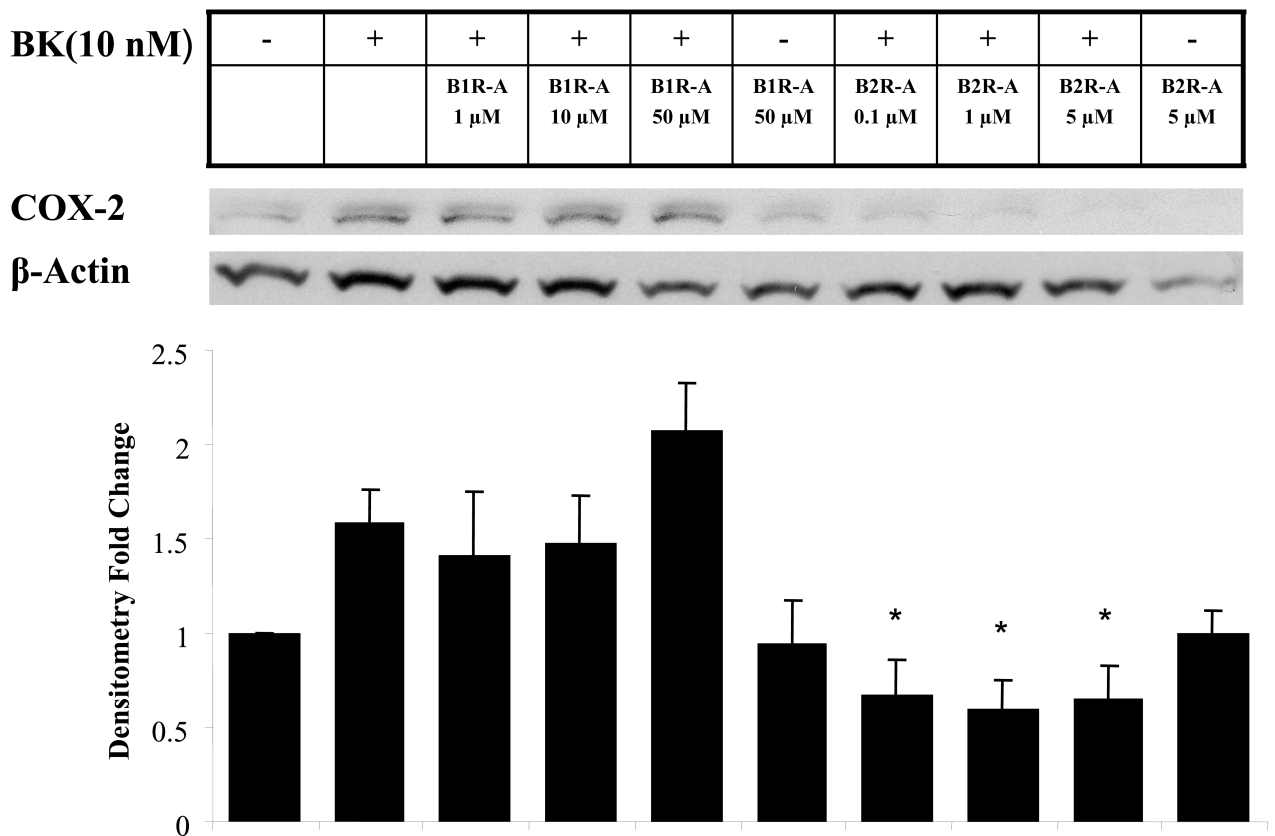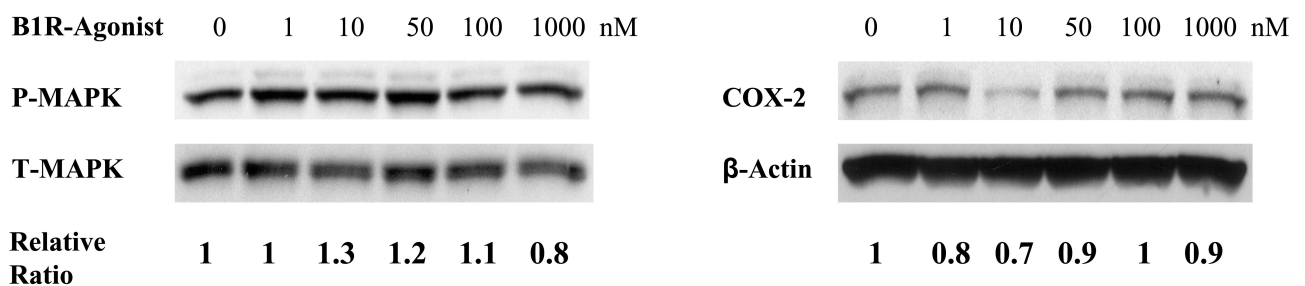BK (nM)   0   0.1   1   10   50   100   200   1000

P-MAPK

T-MAPK

B

Figure 3. BK-induced phosphorylation of MAPK

(A) Dependence of MAPK activation on BK concentration. PCI-37A cells were serum-starved for 48 h, and then treated with increasing concentrations of BK (0.1 - 1000 nM) for 10 min before harvest. (B) Time course of BK-induced p-MAPK. PCI-37A cells were serum-starved for 48 h and then treated with10 nM BK for the indicated time intervals (0 - 8 h). Whole cell lysates were prepared and then immunoblotted with Abs for p-MAPK and total MAPK. Representative immunoblots are shown. The graph presents the fold-change in protein level compared to control as determined by densitometry (cumulative results from three independent experiments) and correlates to the lane shown directly above each bar. Data shown are the mean ± SE. Symbol * indicated $P < 0.05$ as compared with the control.

A

BK	–	10nM	10nM	10nM	10nM	10nM	–	–
Lys-[Leu8]des-Arg9-BK	–	–	1 µM	10 µM	–	–	10 µM	–
HOE140	–	–	–	–	1 µM	10 µM	–	10 µM

IP: EGFR
IB:PY20

IP:EGFR
IB:EGFR

Relative Ratio	1.0	10.3	8.3	13.2	7.7	2.9	0.3	0.4

B

Hoe140   –   –   0.1   1   10   1   µM   B1Rant   –   –   0.1   1   10   1   µM

BK   –   +   +   +   +   –   BK   –   +   +   +   +   –

P- MAPK

T- MAPK

C

BK(10 nM)	-	+	+	+	+	-	+	+	+	-
			B1R-A 1 μM	B1R-A 10 μM	B1R-A 50 μM	B1R-A 50 μM	B2R-A 0.1 μM	B2R-A 1 μM	B2R-A 5 μM	B2R-A 5 μM

COX-2

β-Actin

D

B1R-Agonist	0	1	10	50	100	1000 nM

P-MAPK

T-MAPK

| Relative Ratio | **1** | **1** | **1.3** | **1.2** | **1.1** | **0.8** |

	0	1	10	50	100	1000 nM

COX-2

β-Actin

| **1** | **0.8** | **0.7** | **0.9** | **1** | **0.9** |

Figure 4. BK-induced phosphorylation of EGFR and MAPK and COX-2 expression is mediated through B2 bradykinin receptor but not B1 bradykinin receptor
(A) BK-induced phosphorylation of EGFR in presence of BK receptor antagonists. (B) BK-induced phosphorylation of MAPK in presence of BK receptor antagonists. (C) BK-induced COX-2 expression in presence of BK receptor antagonists. PCI-37A cells were serum-deprived for 3 days, pretreated with a range of concentrations of B1 receptor antagonist Lys-(Des-Arg^9-Leu^8)-BK or B2-receptor antagonist HOE140 as indicated for 1 h, followed by treatment with 50 nM BK for 5 minutes for detection of phospho-EGFR and phospho-MAPK and with 10 nM BK for 2 h for measurement of COX-2. Whole cell lysates were

prepared, and phospho-EGFR, phospho-MAPK, and COX-2 levels were determined by immunoblotting using specific antibodies as described in Materials and Methods. Relative ratios of p-MAPK or COX-2 expression versus total- MAPK or β-Actin expression were calculated. Representative immunoblots are shown. The graph presents the fold-change in protein level compared to control as determined by densitometry (cumulative results from three independent experiments) and correlates to the lane shown directly above each bar. Data are the mean ± SE from two independent experiments. Symbol * shows $P < 0.05$ as compared with BK treatment. (D) Effect of B1R-Agonist on p-MAPK and COX-2 expression. PCI-37A cells were serum-deprived for 2 days, treated with a range of concentrations of B1-agonist Des-Arg[9]- BK for 10 min for p-MAPK (left panel) and 2 h for COX-2 (right panel). Methods used were identical to those described above for Fig. 4 A-C. This is a representative experiment that was repeated two additional times with similar results.

A
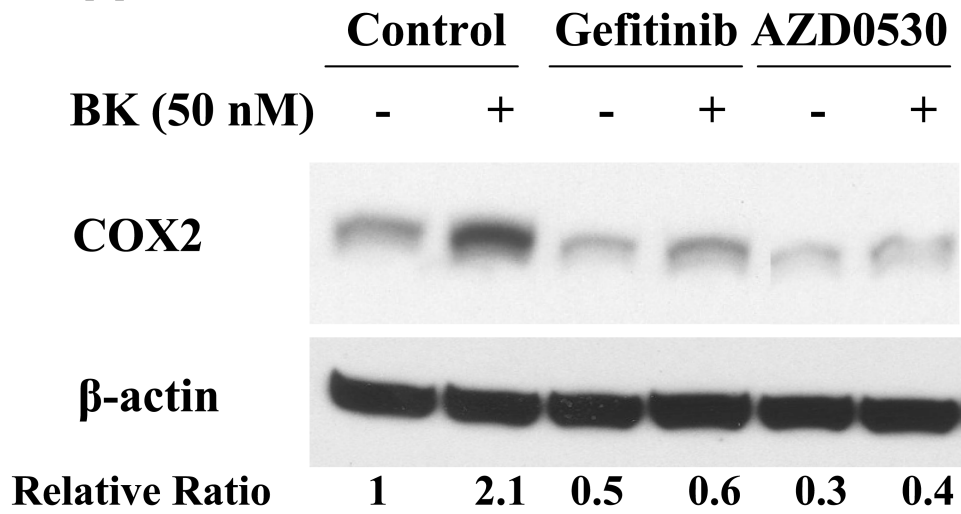
B
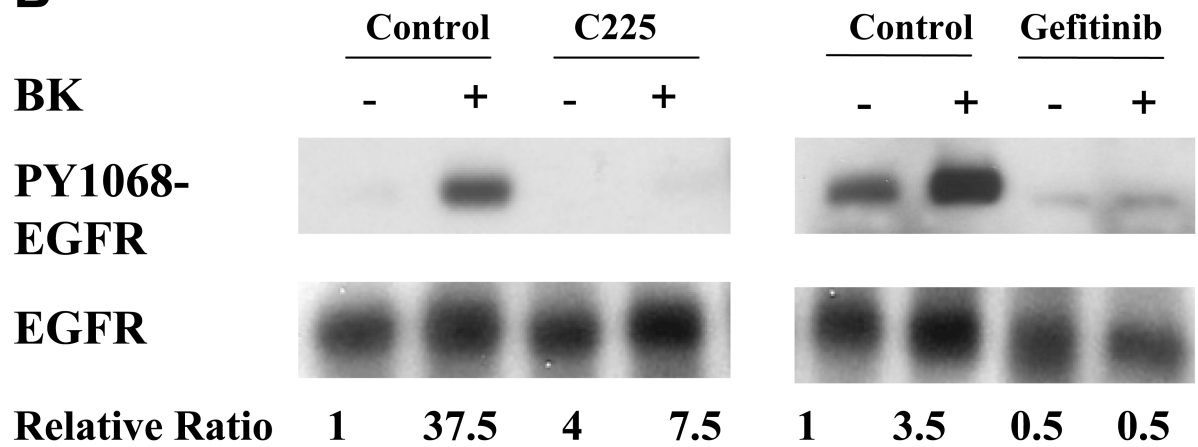
C
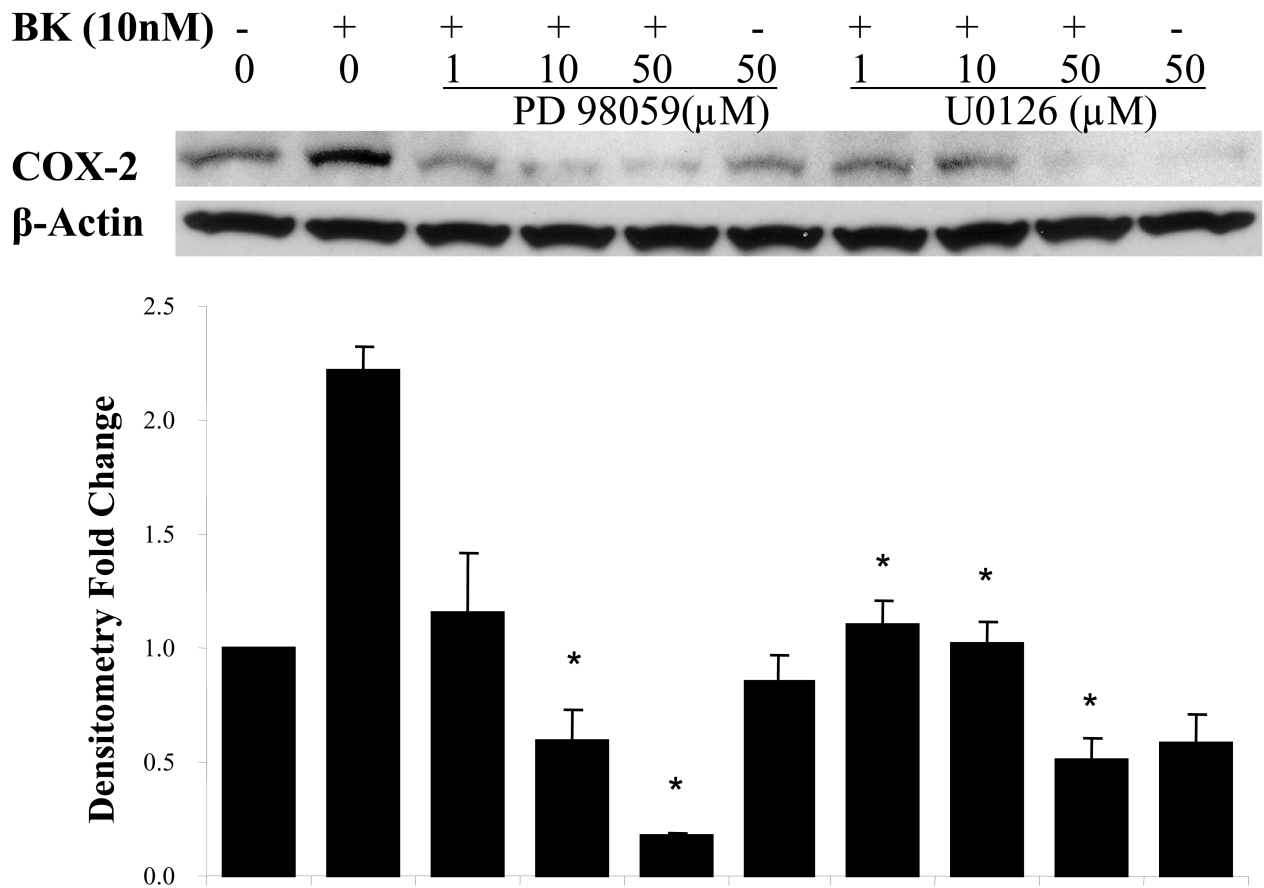
Figure. 5. EGFR and MAPK are required for COX-2 induction by BK
PCI-37A cells were serum-deprived for 3 days followed by subsequent treatments. (A) BK-induced COX-2 expression in presence of an EGFR or a src inhibitor. Cells were pretreated for 60 min with vehicle, the src inhibitor AZD0530 (1 μM) or the EGFR TKI gefitinib (1 μM) followed by treatment with BK (50 nM) for 2 h, and COX-2 protein levels were analyzed by immunoblotting. Relative ratios of COX-2 expression versus β-Actin expression were calculated from two independent experiments. (B) Effect of EGFR inhibition on phosphorylation of EGFR in response to BK. Cells were pre-incubated with vehicle, the EGFR antibody C225 (100nM) or the EGFR TKI gefitinib (1 μM) for 5 min and then treated with BK (50 nM) for 10 min. EGFR phosphorylation at a representative autophosphorylation site Y1068 and total EGFR were analyzed by immunoblotting. Relative ratios of p-EGFR (PY1068) phosphorylation versus total- EGFR were calculated. This is a representative experiment that was repeated two additional times with similar results. (C) BK-induced COX-2 expression in presence of MEK inhibitors. Cells were pretreated with vehicle or MEK inhibitors PD 098059 (1 - 50 μM) or U0126 (1 - 50 μM) for 1 h before treatment with 10 nM BK for another 2 h, and COX-2 expression was determined by immunoblotting with COX-2 antibody. Representative immunoblots are shown. The graph presents the fold-change in protein level compared to control as determined by densitometry (cumulative results from three independent experiments) and correlates to the lane shown

directly above each bar. Data shown are the means $\pm$ SE. Symbol * indicated $P < 0.05$ as compared with the BK treatment.
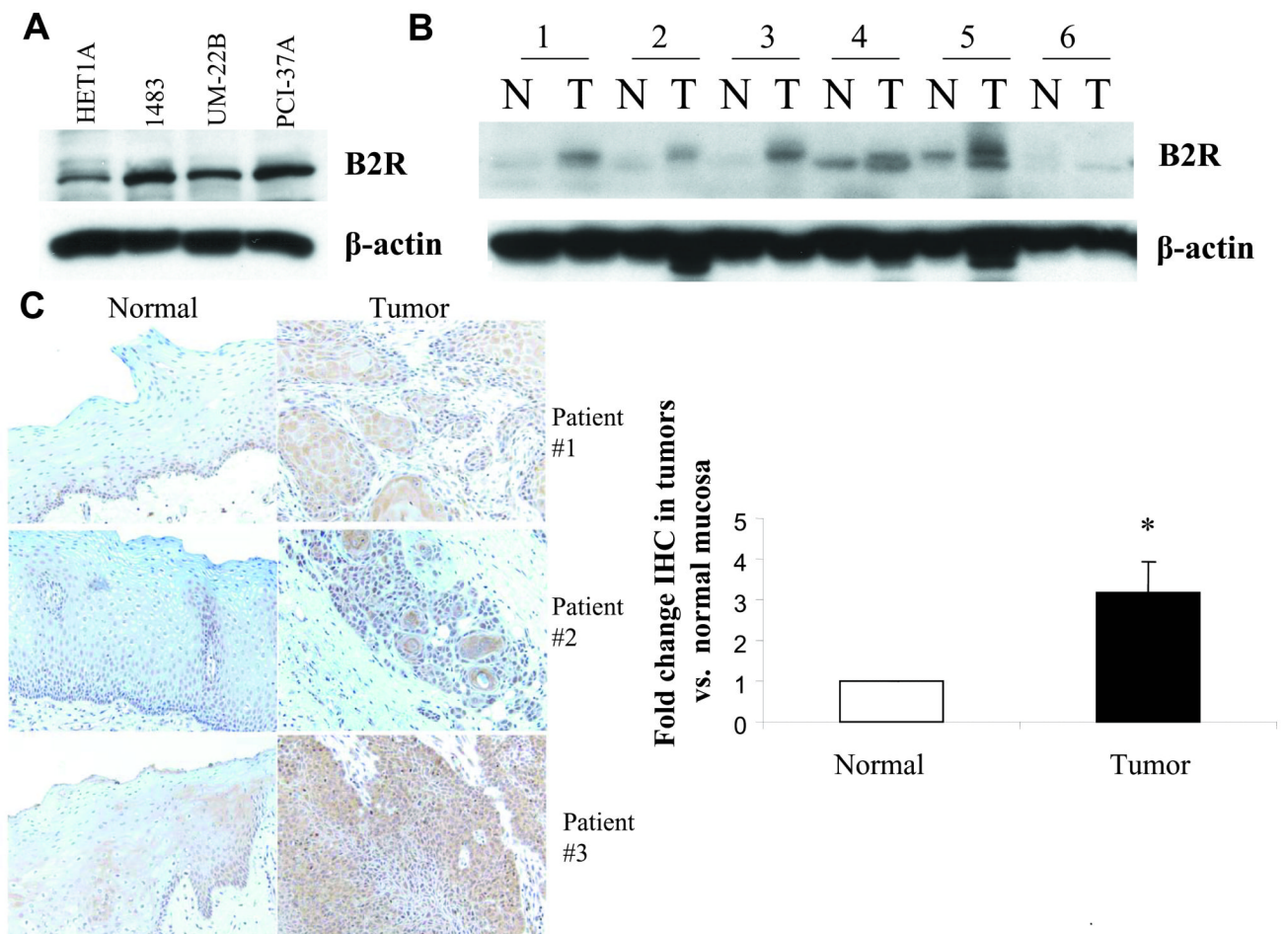
Figure 6. B2 receptor is overpressed in head and neck cancer
(A) HNSCC cell lines. Cell lysates from an immortalized normal mucosa cell line HET1A and three HNSCC cell lines 1483, UM-22B and PCI-37A were subjected to immunoblotblot analysis to determine B2R levels, and then reprobed with beta-actin. (B) HNSCC tumors compared to normal mucosa by immunoblot. Lysates of HNSCC tumors and corresponding control normal mucosa obtained from six patients were probed for B2 receptor levels by immunoblotting and reprobed with beta-actin antibody. (C) Immunohistochemistry (IHC) of B2R expression in tumor tissue compared to normal mucosa from same patient. IHC staining of B2 receptor was performed in tumor tissue and control normal mucosa from 43 HNSCC patients (Tissue sections from three representative patients). The staining intensity was scored as described in 'Materials and Methods' and p-value was computed using the Wilcoxon matched pairs sign rank test.

Table 1

Demographics of HNSCC patients analyzed for B2R staining

Smoking status	N (%)
Smokers	29 (67.4%)
Non-smokers	3 (7%)
Unknown smoking status	11 (25.6%)
Age	
31-40	2 (4.7%)
41-50	5 (11.6%)
51-60	9 (20.9%)
61-70	19 (44.2%)
71-80	7 (16.3%)
81-90	1 (2.3%)
Cancer Type	
Primary	36 (83.7%)
New primary	2 (4.7%)
Recurrence	5 (11.6%)
Race	
Caucasian	40 (93%)
African-American	3 (7%)